Applied Catalysis B: Environmental 232 (2018) 429–435

Contents lists available at ScienceDirect

Applied Catalysis B: Environmental

journal homepage: www.elsevier.com/locate/apcatb

Cyclohexanoic acid breakdown by two-step persulfate and heterogeneous Fenton-like oxidation

Xiyan Xu[a,b,*], Gema Pliego[a], Alicia L. Garcia-Costa[a], Juan A. Zazo[a], Shuming Liu[b], Jose A. Casas[a], Juan J. Rodriguez[a]

[a] Chemical Engineering Section, University Autonoma of Madrid, Crta. Colmenar km 15, 28049, Madrid, Spain
[b] School of Environment, Tsinghua University, 100084, Beijing, China

ARTICLE INFO

Keywords:
Naphthenic acids
Persulfate oxidation
Fenton-like
Activated carbon
γ-Alumina

ABSTRACT

This work reports on the application of a two-step treatment consisting of persulfate (PS) and heterogeneous Fenton-like oxidation for the breakdown of cyclohexanoic acid (CHA, 50 mg L^{-1}) as the model naphthenic acid (NA) of oil sands process affected wastewaters (OSPWs). Home-made activated carbon and γ-alumina-supported iron (Fe/AC and Fe/γ-Al_2O_3) catalysts were tested for the Fenton-like step, namely Catalytic Wet Peroxide Oxidation (CWPO). The two catalysts were compared varying the H_2O_2 dose and temperature on the treatment efficiency and their stability was checked in terms of iron loss by leaching. The catalysts before and after reaction were characterized by 77 K N_2 adsorption-desorption, TXRF and XPS analyses. Results show that over 75% mineralization can be achieved by the combined system at 80 °C. The starting pH was the circumneutral natural value of OSPWs (≈8), which during the PS-oxidation step evolved towards the acid (≈3–3.5), optimum pH for the Fenton-like systems. This, together with the partial substitution of PS by cheaper H_2O_2 and the consequent lower introduction of sulfate into the water are the main advantages of the combined treatment compared to PS-oxidation alone. The time course of TOC in the CWPO step can be well described by pseudo-first and pseudo-second order kinetics for the Fe/AC and Fe/γ-Al_2O_3 catalysts, respectively. Characterization of the fresh and used catalysts shows negligible changes in porous texture for both of the catalysts, while XPS analyses indicate an apparent decrease of the proportion of inorganic oxygen and increase of carboxylic acid group for the AC-based one. That catalyst suffered higher iron leaching and yielded less effective H_2O_2 consumption. The amount of oxalic acid formed, the low pH value of the solution after the PS pretreatment and the metal-support interactions in the catalysts tested are experimentally demonstrated to be the main factors affecting iron leaching.

1. Introduction

NAs constitute a group of persistent compounds commonly present in the oil sand process-affected waters (OSPWs) and the marine environment after oil spilling, including numerous kinds of alkyl-substituted saturated cyclic and noncyclical carboxylic acids as well as their oxygenated species [1,2]. A general chemical formula $C_nH_{2n-z}O_aN_bS_c$ can be given to define NAs, where the O, N and S number of classic NAs are 2, 0 and 0 respectively [2]. The structural complexity of NAs results in acute toxicity towards microorganisms, plants and animals [3–5]. The zero-discharge policies of OSPWs promulgated by various countries require an in situ storage or incorporation into a reclaimed system [6]. However, NAs are so recalcitrant that they can remain in the tailing pounds for over ten years [7].

To mitigate the environmental impact of NAs, physical, biological and chemical approaches have been used. Physical treatments allow NAs separation from the liquid phase but not their decomposition, while biological methods are invalid for certain portion of NAs because of their toxicity [2]. The advanced oxidation processes (AOPs), characterized by the positive effect of reactive radicals [8], draws more and more attention for the treatment of NAs in recent years [9], since these approaches allow the mineralization of the toxic target components. Ozonation[10], chelate-Fenton [11], thermally-activated PS [12], UV/H_2O_2, UV/PS, UV or solar/TiO_2 [13,14], zero valent iron (ZVI) activated PS [15] and UV/Chlorine [16] have been tested for NAs degradation up to now. Our previous work showed the efficiency of thermally-activated PS for the breakdown of model NAs with the positive effect of dissolved oxygen [12].

However, the PS-based oxidation system has apparent drawbacks hindering its potential application, such as the high reagent cost and the

* Corresponding author at: Chemical Engineering Section, University Autonoma of Madrid, Crta. Colmenar km 15, 28049, Madrid, Spain.
E-mail address: xiyanxu@tsinghua.edu.cn (X. Xu).

https://doi.org/10.1016/j.apcatb.2018.03.092
Received 3 January 2018; Received in revised form 22 March 2018; Accepted 25 March 2018
Available online 27 March 2018
0926-3373/

incorporation of sulfate ions into the final effluent. Fenton oxidation is recognized as one of the most cost-effective AOPs [8]. Nonetheless, investigation of Fenton-based processes for the abatement of NAs has been scarce so far [11,15,17]. It has to be considered that the natural pH of OSPWs is around 8 and the iron ions tend to form complexes with NAs even if the pH is artificially adjusted to optimum (≈3–3.5). Chelate-Fenton oxidation working at circumneutral pH has been used for the breakdown of CHA to prevent the precipitation of iron ions [18], but the radical-scavenging effect and possible toxicity derived from the chelate reagents should be addressed for practical use. In addition, conventional homogeneous Fenton oxidation suffers of the continuous iron loss with the effluent and the subsequent need of dealing with the sludge resulting from $Fe(OH)_3$ precipitation upon neutralization previous to discharge [19].

The combination of thermally-activated PS and heterogeneous Fenton-like oxidation, namely catalytic wet peroxide oxidation (CWPO), could be applied for the breakdown of CHA since it allows overcoming the drawbacks of both PS oxidation and conventional Fenton [20,21]. The PS oxidation step allows pre-decomposition of CHA to avoid the formation of Fe-NA complexes and reduces the pH down to the optimum (≈3) for the following Fenton step due to the generation of large amount of protons [22]. The following CWPO step, on the other hand, would effectively reduce the reagent cost by substituting part of the PS amount by significantly cheaper H_2O_2. Meanwhile, the iron loss would be avoided or drastically reduced with respect to conventional homogeneous Fenton.

Fe catalysts supported on activated carbon (Fe/AC) [23] and γ-alumina (Fe/γ-Al_2O_3) [24,25] are among the most commonly used for heterogeneous Fenton. The former has been also studied as catalyst itself for H_2O_2 decomposition upon thermal-activation [26]. Leaching of the metallic phase is one of the main causes of catalyst decay limiting potential application. Previous investigations showed that oxalic acid resulting from the oxidation of organic pollutants is a main responsible of that iron leaching [23]. Besides, the metal-support interactions are also crucial. Metals can connect directly to the different sites on the carbon surface or corresponding surface groups [27,28], while they tend to connect with γ-Al_2O_3 in a particular coordinated manner to form a relatively strong link [29]. However, there is still a lack of available information on the comparison between these two commonly used supports in iron catalysts for CWPO.

In the current work, a two-step PS and heterogeneous Fenton-like oxidation system is applied for the first time for the abatement of CHA as the model NA, in aqueous phase. Home-made Fe/AC and Fe/γ-Al_2O_3 are tested as catalysts for the Fenton-like step, making a comparison of their performance in terms of activity and stability.

2. Materials and methods

2.1. Materials

Incipient wetness impregnation was used for the preparation of the home-made Fe/AC [23] and Fe/γ-Al_2O_3 [30] catalysts. AC and γ-Al_2O_3 with particle diameter less than 100 μm from Merck (Germany) were impregnated by $Fe(NO_3)_3{\cdot}9H_2O$ solution to adjust the Fe load at nominal 4% (w/w). After left in room condition for 2 h, the impregnated samples were dried for 12 h at 60 °C and then calcined at 300 °C for 4 h. CHA and other reagents used in the current study were all purchased from Sigma-Aldrich with purification over 98%.

2.2. Experimental

The oxidation experiments were carried out batchwise in 100 mL glass bottle using 50 mL of 50 mg L^{-1} CHA solution. The samples were preheated in water bath at 60–97 °C and shaken at equivalent 200 rpm. PS was added at 20% of the stoichiometric dose [12] and the reaction was maintained for 2 h. In this step, the pH of the solution dropped from 8 to 3. Then H_2O_2 was added in different amounts (20–80% of the stoichiometric referred to complete oxidation of the starting CHA). The catalyst was incorporated at 250 mg L^{-1}, and different reaction times were maintained, after which samples were taken, filtered and immediately analyzed. The results shown are the averages of duplicates.

2.3. Analytical methods

Total organic carbon (TOC) was measured in a TOC analyzer (Shimadzu, mod. TOC, VSCH). Iron concentration in the solution was determined following the o-phenantroline method [31]. The concentration of PS was measured by a spectrophotometric method based on modification of the iodometric titration analysis [32]. The H_2O_2 concentration was determined using the titanium sulfate method [33]. Short-chain carboxyl acids were analyzed by ionic chromatography with chemical suppression (Metrohm 790 IC equipped with a conductivity detector). A Metrosep A supp 5–250 column (25 cm length, 4 mm i.d.) was used as stationary phase and the mobile phase consisted of 3.2 mM Na_2CO_3 and 1 mM of $NaHCO_3$ at pumping rate of 0.7 mL min^{-1}.

2.4. Characterization of the catalysts

The iron content of the fresh and used catalysts was determined by total reflection X-ray fluorescence (TXRF), using a TXRF spectrometer 8030c. The BET area, pore volume and micropore size were measured by N_2 adsorption-desorption at 77 K using a Micromeritics Tristar 3020 apparatus. The samples were previously degassed overnight at 150 °C to a residual pressure of 10^{-5} Torr [34]. The BET surface area (S_{BET}) was calculated using the Brunauer–Emmett–Teller (BET) equation. The t-plot method was used to calculate the micropore area (S_{Micro}) and micropore volume (V_{Micro}). The total pore volume (V_{Total}) was assessed from the amount of N2 adsorbed at $P/P_0 = 0.99$. X-ray photoelectron spectra (XPS) were recorded with a VGEscalab 200R spectrometer equipped with a Kα Thermo Scientific apparatus with an Al Kα ($h\nu$ = 1486.68 eV) X-ray source using a voltage of 12 kV under vacuum (2×10^{-7} mbar) condition [35]. Binding energies were calibrated according to the C 1 s peak of carbon samples at 284.6 eV. For the analysis of the peaks, a Shirley type background was used. Peaks were adjusted to a combination of Gaussian and Lorentzian functions using the XPS Peak 4.1 software [36].

3. Results and discussion

Before testing the two-step system, heterogeneous Fenton the AC- and γ-Al_2O_3-supported catalysts were carried out. Less than 40% mineralization was achieved after 6 h with as much as the stoichiometric amount of H_2O_2. As indicated before, the complexation of surface Fe by CHA must be a main cause of that poor result.

Then, the two-step approach was tested with 20% of the stoichiometric amount of PS in a first 2 h-step followed by CWPO with different amounts of H_2O_2 for another 4 h, using 250 mg L^{-1} of catalyst. The working temperature was 80 °C in both steps. As can be seen in Fig. 1, PS oxidation under the above conditions allowed around 40% TOC reduction and the later CWPO step gave rise to significant further mineralization, depending on the H_2O_2 amount and the catalyst used. Previous adsorption experiments were performed with the effluent from the PS step and the two catalysts tested, in absence of H_2O_2 and the results showed that the contribution of adsorption to TOC removal can be neglected. In the first oxidation step, PS gives rise to $SO_4^{\cdot -}$ radicals which can degrade and partially mineralize CHA with the positive effect of $O_2^{\cdot -}/HO_2$ radicals derived from dissolved oxygen [12]. Pre-degradation of CHA hinders Fe complexation in the following Fenton-like step. Meanwhile, the reactions involved in PS oxidation produce an important release of protons causing pH reduction up to ≈3, recognizing as the optimum for Fenton. Looking at the two catalysts, the

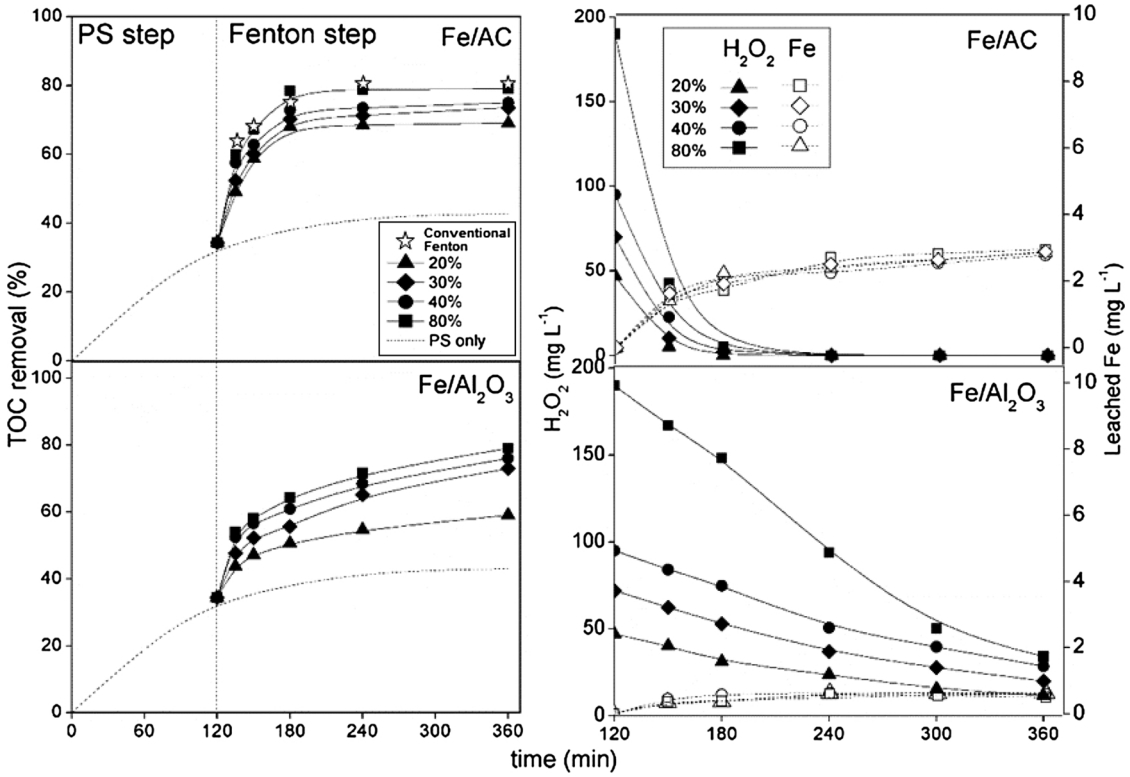

Fig. 1. Time-course of TOC, H_2O_2 and leached Fe upon the two-step PS(2 h) and CWPO(4 h) with the catalysts tested at different H_2O_2 doses (% of the stoichiometric). [PS] = 20% of the stoichiometric, [catalysts] = 250 mg L^{-1}; pentagrams stand for the TOC removal of CHA by two-step PS (20% of the stoichiometric) and conventional Fenton oxidation (40% of the stoichiometric H_2O_2 + 10 mg L^{-1} of Fe^{2+}); pH_0 = 8; T = 80 °C.

AC-supported yielded faster and slightly higher mineralization. That can be attributed to a faster HO generation upon H_2O_2 decomposition, due in part to higher iron leaching, since about 3 mg L^{-1} were analyzed in the liquid phase with Fe/AC versus no more than 0.3 mg L^{-1} with Fe/γ-Al_2O_3. Therefore, the results cannot be used to prove an obvious higher activity of the Fe/AC catalysts since the contribution of homogeneous reaction can be some significance in its case while much less important with Fe/γ-Al_2O_3.

As observed in Fig. 1, increasing the H_2O_2 dose improves TOC reduction although above 30% of the stoichiometric that effect becomes of lower relative importance. The remaining TOC corresponded to short-chain organic acids like oxalic, formic and acetic. The results of CHA mineralization by two-step PS (20% of the stoichiometric) and conventional Fenton oxidation (40% of the stoichiometric H_2O_2 + 10 mg L^{-1} of Fe^{2+}) have also been included in the figure. As can be seen, the final TOC removal by that system is only around 5% higher than by heterogeneous Fenton. Thus, the later shows a better applicability due to much lower iron loss. Comparing the two catalysts, iron leaching from the AC-supported catalyst was significantly higher than the observed with the γ-Al_2O_3 one, which means a higher stability of this last and a lower contribution of homogeneous Fenton. The difference of iron leaching between the two catalysts must be due to the corresponding discrepancy of their metal-support interaction.

Other working temperatures were tested (60 and 97 °C) and the results are shown in Fig. 2. Compared with the results of Fig. 1, it can be seen that increasing the temperature from 80 to 97 °C has no significant and even some small negative effect on the extent of mineralization, which is due to enhanced radical scavenging at the highest temperature [37]. H_2O_2 decomposed more rapidly at that temperature, especially with Fe/AC, where it was consumed completely within 30 min (Fig. 2). On the other hand, no significant difference of iron leaching was found between 80 and 97 °C. A dramatic decrease of mineralization occurred at 60 °C in both the PS and CWPO steps. That temperature is too low for PS activation and moreover, the lower stent of reaction effects to the evolution of pH, so that at the start of CWPO the pH was around 4.5, above the optimum for Fenton-based oxidation.

Finally, the remaining concentrations of organic acids at the end of the experiments confirm the resistance of acetic and most in particular oxalic acid to Fenton-based oxidation at the temperature tested. Formation of iron(III)-oxalate complex to prevent further mineralization [23,38]. At 80 and 97 °C, the measured residual TOC is almost equal to the corresponding identified organic acids, whereas significant differences were found at 60 °C, indicating the existence of other unidentified reaction byproducts at this temperature, which may have some significance in terms of toxicity.

3.1. Kinetic analysis

TOC-based kinetic analysis has been conducted to learn on the rate of mineralization of organic pollutants [12,20,22,39]. The rate of NAs mineralization with PS has been well described by simple pseudo-first-order kinetics [12]. The pseudo-first-order rate equation has been applied for describing the degradation of organic pollutants by heterogenous Fenton [40] and other catalytic oxidation systems [22,41], while pseudo-second-order kinetics has been used for homogenous Fenton system in the literature [8]. This last is more similar the case of Fe/AC system in the current study, since homogeneous Fenton oxidation takes an important role due to the higher iron leaching. Therefore, the following rate equations have been used to describe the kinetics of CHA mineralization in the CWPO step:

$$-\frac{d[TOC]}{dt} = k_1[TOC]^2[H_2O_2] \quad (Fe/AC)$$

$$-\frac{d[TOC]}{dt} = k_1[TOC][H_2O_2] \quad (Fe/\gamma - Al_2O_3)$$

while the evolution of H_2O_2 follows the first order [30]:

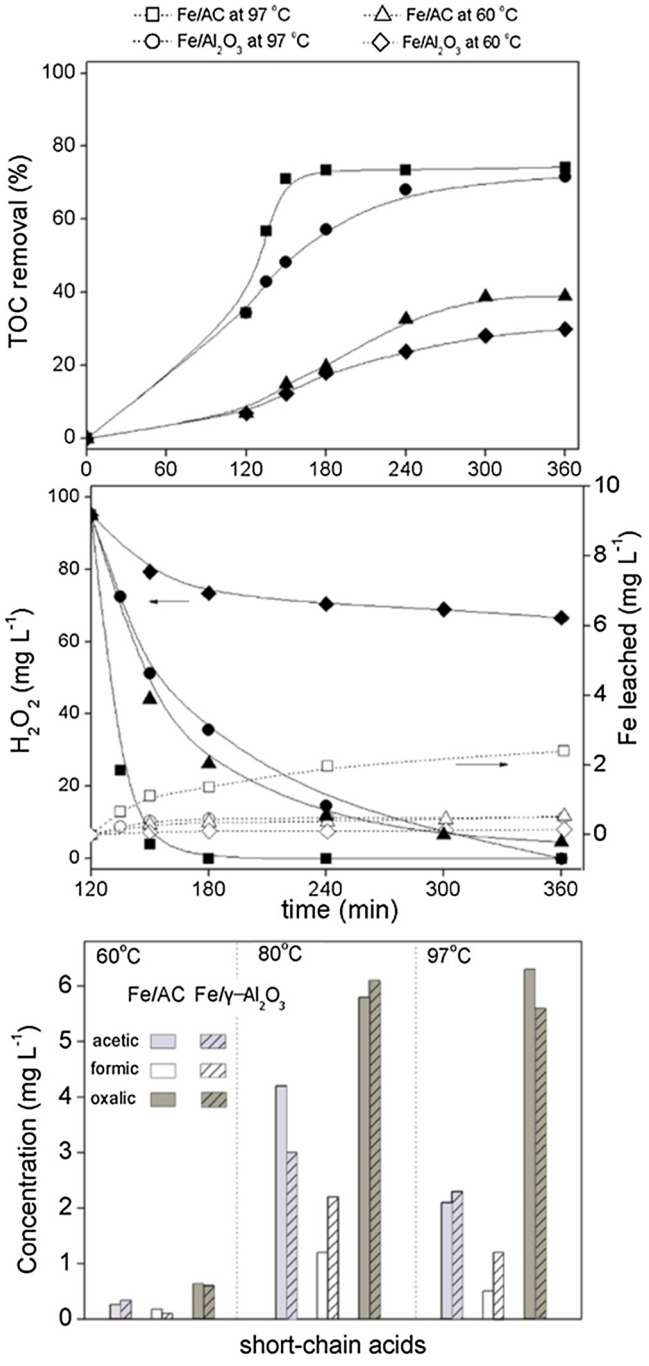

Fig. 2. Time-course of TOC, H_2O_2 and leached Fe (open symbols) and final concentrations of short-chain organic acids upon PS(2 h)-CWPO(4 h) with the catalysts tested at different temperatures: PS and H_2O_2 at 20 and 40% of the stoichiometric, respectively; [catalysts] = 250 mg L^{-1}; pH_0 = 8; T = 80 °C.

$$-\frac{d[H_2O_2]}{dt} = k_2[H_2O_2]$$

Fitting the experimental values of TOC and H_2O_2 concentration upon reaction time with the Fe/AC and Fe/γ-Al_2O_3 catalysts at different H_2O_2 doses and temperatures provided the values of the kinetic constants summarized in Table 1. The values of the regression coefficient are indicative of good fitting, which can be confirmed from the curves of Fig. 2 (branches corresponding to the heterogeneous Fenton step). Although the values of k_2 (H_2O_2 decomposition) are one order of magnitude higher for the Fe/AC catalysts, this does not imply a higher intrinsic activity, since, as indicated before, there must be in this case some significant contribution of homogeneous reaction derived from iron leaching.

3.2. Effect of chloride

The effect of chloride was considered, since the OSPWs contain in general fairly high concentrations of that species [15] which has been recognized as a potential scavenger of $HO^{\bullet}$ radicals [42–44]. Some negative effects, on PS oxidation of NAs were reported in our previous work [12]. In the current study, sodium chloride was added at 10 g L^{-1} to analyze its effect on the two-step system investigated, using 20 and 40% of the stoichiometric PS and H_2O_2, respectively, with 250 mg L^{-1} catalyst in the CWPO step. Under these conditions, despite similar H_2O_2 decomposition (compared to that without scavenger) TOC removal was reduced by around 20% with both catalysts after 6 h of reaction, confirming the scavenging effect of chloride. It has been reported that chloride might even provoke the formation of organochlorinated species in advanced oxidation [15]. Therefore, the effect of chloride needs to be taken into account regarding the potential application of the current PS-CWPO approach as has been reported for other AOP systems [42–44].

3.3. Stability of the catalysts

The catalysts tested were separated after reaction and used again after simply drying, under the same conditions. As shown in Fig. 3, the extent of mineralization decreased more significantly upon successive uses in the case of the AC-supported catalyst. This must be due to its higher iron loss by leaching. About 60% mineralization was still achieved after 7 cycles, with 77.6% and 44.3% overall iron loss from the Fe/AC and Fe/γ-Al_2O_3 catalysts, respectively. These results prove a somewhat better stability of the γ-Al_2O_3-supported catalyst, although further research efforts need to be done to improve this crucial issue for potential application.

On the other hand, it can be seen in Fig. 3 that less significant differences were observed for mineralization than for H_2O_2 consumption between the two catalysts upon successive uses and, opposite to TOC reduction, H_2O_2 conversion decreased more rapidly in the case of the γ-Al_2O_3-supported one. This can be explained by the fact that AC promotes in some extent H_2O_2 decomposition into O_2 (plus H_2O_2), ineffective under the operating conditions of the current work [36]. Also, the parasitic scavenging of $HO^{\bullet}$ radicals can be more pronounced in the case of Fe/AC due to the higher iron concentration in the liquid phase [45]. Therefore, the Fe/γ-Al_2O_3 catalyst allows more efficient consumption of H_2O_2.

With regard to the causes of iron leaching, it has been reported that oxalic acid formed as oxidation byproduct is a main responsible [23,46]. Experiments were carried out to further explore the effect of oxalic acid on iron leaching from the two catalysts tested. They were stirred for 6 h in contact with aqueous solutions of oxalic acid of different concentration at 80 °C. The results are shown in Fig. 4. Blank experiments at pH = 3 without oxalic acid were previously performed yielding 0.64 and 0.09 mg L^{-1} of iron leached from the Fe/AC and Fe/γ-Al_2O_3 catalysts, respectively (Fig. 4). As can be seen, increasing the oxalic acid concentration enhances iron leaching, confirming its significant impact. However, fairly important differences can be observed between the two catalysts. Therefore, the specific metal-support interaction must play an important role in that respect.

3.4. Characterization of the fresh and used catalysts

To learn more on the oxidation processes involved and the causes of deactivation of the catalysts tested, they have been characterized by different techniques before and after use in CWPO.

The 77 K N_2 adsorption-desorption isotherms are shown in Fig. 5. As

Table 1
Values of the rate constants for CHA mineralization and H_2O_2 decomposition upon heterogeneous Fenton oxidation catalyzed by Fe/AC and Fe/γ-Al_2O_3 at different conditions.

H_2O_2 (% stoi.)	T (°C)	Fe/AC				Fe/γ-Al_2O_3			
		$k_1 \times 10^5$ L^2 mg^{-1} min^{-1}	R^2	$k_2 \times 10^2$ min^{-1}	R^2	$k_1 \times 10^6$ L mg^{-2} min^{-1}	R^2	$k_2 \times 10^3$ min^{-1}	R^2
20	80	2.26 ± 0.50	0.99	5.34 ± 0.14	0.99	3.97 ± 1.59	0.99	5.82 ± 0.36	0.99
30	80	2.98 ± 0.66	0.98	5.59 ± 0.53	0.97	4.33 ± 1.70	0.99	5.03 ± 0.21	0.99
	60	0.31 ± 0.08	0.99	2.19 ± 0.14	0.98	0.68 ± 0.21	0.99	1.95 ± 0.26	0.99
40	80	3.57 ± 0.74	0.99	5.67 ± 0.29	0.99	5.09 ± 0.13	0.99	4.86 ± 0.17	0.99
	97	5.85 ± 0.67	0.98	9.27 ± 0.32	0.99	8.58 ± 1.87	0.99	17.6 ± 0.71	0.99
80	80	5.53 ± 0.76	0.99	6.23 ± 0.40	0.99	5.83 ± 0.68	0.99	5.96 ± 0.22	0.99

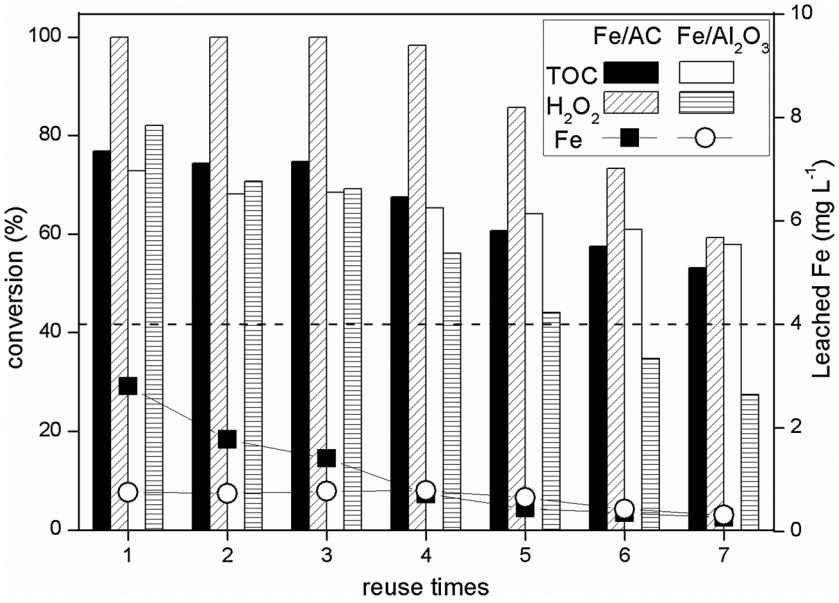

Fig. 3. Performance of the catalysts tested upon successive uses. Mineralization achieved by PS oxidation is given by the dash line (42.0%): [H_2O_2] = 40% of the stoichiometric; [catalysts] = 250 mg L^{-1}; reaction time = 2 h (PS) + 4 h (CWPO); pH_0 = 8; T = 80 °C).

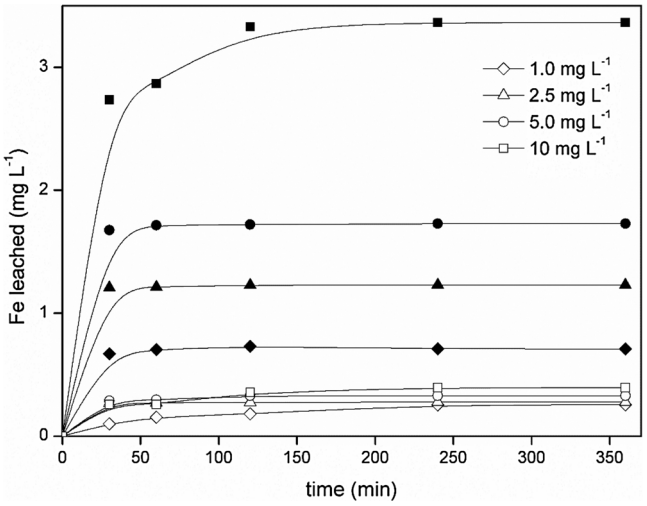

Fig. 4. Effect of oxalic acid on iron leaching from the Fe/AC (solid symbols) and Fe/γ-Al_2O_3 (open symbols) catalysts. pH = 3; T = 80 °C.

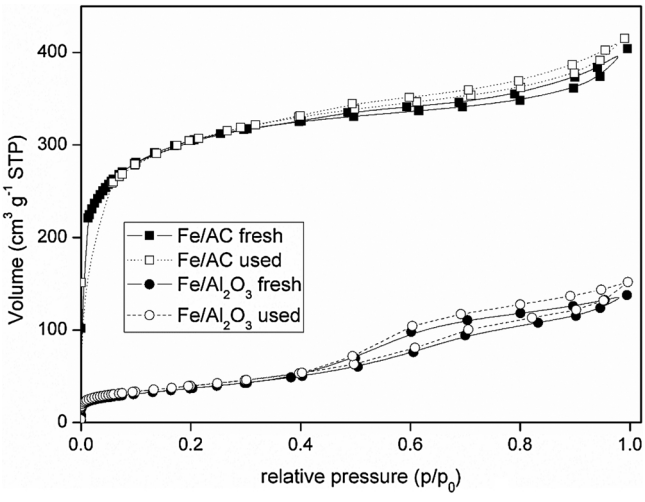

Fig. 5. 77 K N_2 adsorption-desorption isotherms of the fresh and used catalysts.

expected, the Fe/AC catalyst showed much higher adsorption than the Fe/γ-Al_2O_3 one, given the higher BET surface area of the activated carbon support, which is an essentially microporous solid while γ-Al_2O_3 is a mesoporous one. No significant changes were observed in the used catalysts respect to the corresponding fresh ones as confirmed by the representative values of the porous texture summarized in Table 2.

The fresh and used catalysts were characterized also by XPS and the corresponding profiles are shown in Fig. 6. Table 3 summarizes the information on the nature and relative amounts of surface oxygen groups (SOGs) assessed from the O 1 s spectra. In the fresh and used AC-supported catalysts, four symmetric peaks at binding energy values of 530.0, 531.5, 532.9 and 534 eV were obtained from deconvolution of the spectra. Following the criteria used in the literature [36,47,48],

Table 2
Characterization of the porous texture of the fresh and used catalysts.

Catalysts		S_{BET} ($m^2 g^{-1}$)	S_{Micro} ($m^2 g^{-1}$)	V_{Total} ($cm^3 g^{-1}$)	V_{Micro} ($cm^3 g^{-1}$)	D_{Ave} (nm)
Fe/AC	fresh	1026	903	0.62	0.43	2.4
	used	1011	845	0.64	0.41	2.5
Fe/γ-Al_2O_3	fresh	133	–	0.21	–	6.4
	used	139	–	0.23	–	6.6

Table 3
SOG assessment from deconvolution of the O 1 s region of the XPS.

Peak position (eV)	Assessed SOGs	Proportion (%)	
Fe/AC		Fresh	used
530	O–Fe; O–In[a]	42.9	4.0
531.5	C═O	45.9	44.5
532.9	C—O	3.2	13.2
534	COOH	8.1	25.0
536	Ads. water	n.d.	13.3
Fe/γ-Al_2O_3			
530.4	Al_2O_3	75.7	32.7
531.3	S—O	n.d.	8.5
531.5	O—H	n.d.	33.5
531.95	Fe_2O_3	24.3	25.3

[a]In: Inorganic impurities from the ash content of AC support.
n.d.: not deconvoluted.

those groups were assessed to the oxygen of the inorganic matter, C═O bonds associated to carbonyl or quinone groups, C—O bonds of phenol, anhydride or ether groups and carboxylic acid groups, respectively, An additional symmetric peak at 536.0 eV can be observed in the used catalyst, simply assessed to adsorbed water [36,49].

The CWPO process decreased the proportion of inorganic oxygen bonds, like Fe—O on the surface of the Fe/AC catalyst, consistently with the iron leaching. An significant increase of carboxylic acid group was observed, which are believed to be the sites for ineffective decomposition of H_2O_2 [36]. Regarding to the alumina-supported catalyst, the symmetric peaks at 530.4 and 531.95 eV are associated with the oxygen bonds of Fe/γ-Al_2O_3 [50] and Fe_2O_3 [51], respectively. One more peak at 531.3 eV in the used catalyst may correspond to sulfur-oxygen (S—O) bonds of adsorbed sulfate remaining from the PS step [52].

The results of the TXRF analyses showed that the percentage of Fe in the Fe/AC and Fe/γ-Al_2O_3 used catalysts decreased to 3.1% and 3.7%, respectively versus the original 4%, supporting the higher iron loss from the former. This can also be confirmed by the significantly decreased Fe 2 p region of the XPS spectra of Fe/AC after use (Fig. 6). In addition, it can be observed that the bonding energy of the characteristic peaks of Fe 2 p spectra of the two catalysts differ slightly from 711.3, 719.0 and 724.5 eV for the AC-supported catalyst [36] to 710.6, 718.8 and 724.1 eV, respectively, for the γ-Al_2O_3 one [30]. This must suggest some differences in metal-support interactions between the two catalysts.

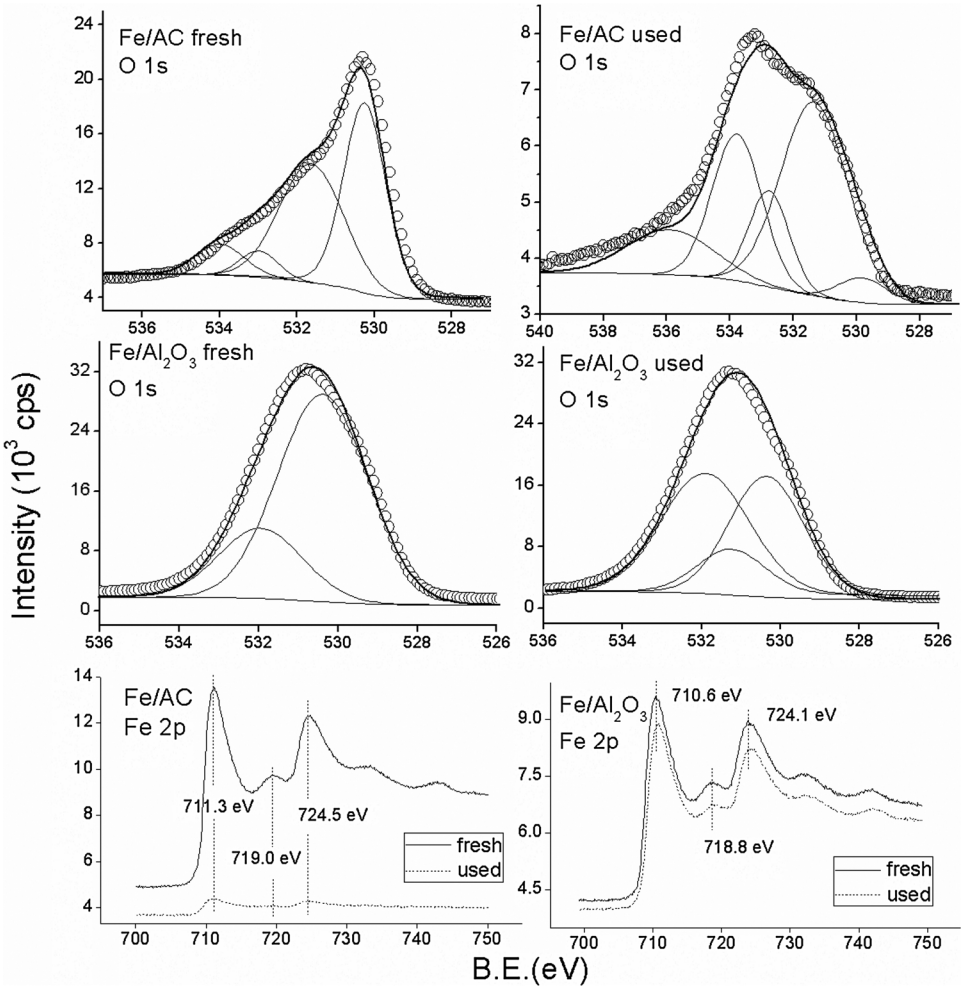

Fig. 6. O 1 s and Fe 2p XPS profiles of the fresh and used catalysts.

4. Conclusions

In the current work, a two-step treatment consisting of PS oxidation followed by heterogeneous Fenton like oxidation (CWPO) has been investigated for the breakdown of CHA as model NA. In the CWPO step, home-made Fe/AC and Fe/γ-Al_2O_3 catalysts were tested. Over 75% final TOC removal has been achieved at 80 °C, using 20 and 30% of the stoichiometric amount of PS and H_2O_2, respectively. The evolution of mineralization upon the CWPO step can be well described by pseudo-second for the AC-supported and pseudo-first for the other. The AC-supported catalyst provides an enhanced H_2O_2 decomposition but with less effective production of hydroxyl radicals than the γ-Al_2O_3-supported one, due to the presence of some oxygen surface groups (mainly carboxylic acid) as confirmed by XPS analyses. Moreover, the AC-supported catalyst suffered higher iron leaching on account of weaker metal-support interaction. Other factors like the concentration of oxalic acid and the acidity of the solution are also responsible for the iron loss from the catalysts.

Acknowledgements

Chinese scholarship council (CSC) is grateful for the support of the doctoral project of Xiyan Xu (File No. 201308410047); We are also grateful for the financial support of Spanish MINECO through project CTQ2013-41963-R.

References

[1] B. Wang, Y. Wan, Y. Gao, M. Yang, J. Hu, Environ. Sci. Technol. 47 (2013) 9545–9554.
[2] P.J. Quinlan, K.C. Tam, Chem. Eng. J. 279 (2015) 696–714.
[3] R.A. Frank, K. Fischer, R. Kavanagh, B.K. Burnison, G. Arsenault, J.V. Headley, K.M. Peru, G. Van der Kraak, K.R. Solomon, Environ. Sci. Technol. 43 (2009) 266–271.
[4] X. Zhang, S. Wiseman, H. Yu, H. Liu, J.P. Giesy, M. Hecker, Environ. Sci. Technol. 45 (2011) 1984–1991.
[5] K.E. Tollefsen, K. Petersen, S.J. Rowland, Environ. Sci. Technol. 46 (2012) 5143–5150.
[6] L.A. Leclair, L. Pohler, S.B. Wiseman, Y. He, C.J. Arens, J.P. Giesy, S. Scully, B.D. Wagner, M.R. van den Heuvel, N.S. Hogan, Environ. Sci. Technol. 49 (2015) 5743–5752.
[7] P.R. Kannel, T.Y. Gan, J. Environ. Sci. Health A Tox. Hazard. Subst. Environ. Eng. 47 (2012) 1–21.
[8] J.A. Zazo, J.A. Casas, A. Mohedano, M.A. Gilarranz, J.J. Rodriguez, Environ. Sci. Technol. 39 (2005) 9295–9302.
[9] X. Xu, G. Pliego, J.A. Zazo, S. Sun, P. García-Muñoz, L. He, J.A. Casas, J.J. Rodriguez, Crit. Rev. Environ. Sci. Technol. 47 (2017) 1337–1370.
[10] E. Garcia-Garcia, J.Q. Ge, A. Oladiran, B. Montgomery, M.G. El-Din, L.C. Perez-Estrada, J.L. Stafford, J.W. Martin, M. Belosevic, Water Res. 45 (2011) 5849–5857.
[11] Y. Zhang, N. Klamerth, P. Chelme-Ayala, M. Gamal El-Din, Environ. Sci. Technol. (2016).
[12] X. Xu, G. Pliego, J.A. Zazo, J.A. Casas, J.J. Rodriguez, J. Hazard. Mater. 318 (2016) 355–362.
[13] X. Liang, X. Zhu, E.C. Butler, J. Hazard. Mater. 190 (2011) 168–176.
[14] T. Leshuk, T. Wong, S. Linley, K.M. Peru, J.V. Headley, F. Gu, Chemosphere 144 (2016) 1854–1861.
[15] P. Drzewicz, L. Perez-Estrada, A. Alpatova, J.W. Martin, M.G. El-Din, Environ. Sci. Technol. 46 (2012) 8984–8991.
[16] Z. Shu, C. Li, M. Belosevic, J.R. Bolton, M.G. El-Din, Environ. Sci. Technol. 48 (2014) 9692–9701.
[17] Y. Zhang, N. Klamerth, S.A. Messele, P. Chelme-Ayala, M.G. El-Din, J. Hazard. Mater. 318 (2016) 371–378.
[18] Y. Zhang, J. Xue, Y. Liu, M.G. El-Din, Chem. Eng. J. 302 (2016) 485–497.
[19] H. Li, Y. Li, L. Xiang, Q. Huang, J. Qiu, H. Zhang, M.V. Sivaiah, F. Baron, J. Barrault, S. Petit, J. Hazard. Mater. 287 (2015) 32–41.
[20] X. Xu, G. Pliego, J.A. Zazo, S. Liu, J.A. Casas, J.J. Rodriguez, J. Chem. Technol. Biotechnol. (2018), http://dx.doi.org/10.1002/jctb.5569 in press.
[21] C.S. Rodrigues, O. Soares, M. Pinho, M.F. Pereira, L.M. Madeira, Appl. Catal. B Environ. 219 (2017) 109–122.
[22] X.-Y. Xu, G.-M. Zeng, Y.-R. Peng, Z. Zeng, Chem. Eng. J. 200 (2012) 25–31.
[23] J.A. Zazo, J.A. Casas, A.F. Mohedano, J.J. Rodríguez, Appl. Catal. B Environ. 65 (2006) 261–268.
[24] M. Munoz, Z.M. de Pedro, J.A. Casas, J.J. Rodriguez, Water Res. 47 (2013) 3070–3080.
[25] P. Bautista, A. Mohedano, N. Menéndez, J.A. Casas, J.J. Rodríguez, Catal. Today 151 (2010) 148–152.
[26] C.M. Domínguez, A. Quintanilla, P. Ocón, J.A. Casas, J.J. Rodriguez, Carbon 60 (2013) 76–83.
[27] G.G. Wildgoose, C.E. Banks, R.G. Compton, Small 2 (2006) 182–193.
[28] I. Efremenko, M. Sheintuch, J. Catal. 214 (2003) 53–67.
[29] J.H. Kwak, J. Hu, D. Mei, C.-W. Yi, D.H. Kim, C.H. Peden, L.F. Allard, J. Szanyi, Science 325 (2009) 1670–1673.
[30] M. Munoz, Z.M. de Pedro, N. Menendez, J.A. Casas, J.J. Rodriguez, Appl. Catal. B Environ. 136 (2013) 218–224.
[31] E.B. Sandell, Interscience Publishers: New York (1959).
[32] C. Liang, C.-F. Huang, N. Mohanty, R.M. Kurakalva, Chemosphere 73 (2008) 1540–1543.
[33] G. Eisenberg, Ind. Eng. Chem. Anal. Ed. 15 (1943) 327–328.
[34] J. Palomar, J. Lemus, M.A. Gilarranz, J.J. Rodriguez, Carbon 47 (2009) 1846–1856.
[35] A. Rey, P. Garcia-Munoz, M.D. Hernandez-Alonso, E. Mena, S. Garcia-Rodriguez, F.J. Beltran, Appl. Catal. B Environ. 154 (2014) 274–284.
[36] A. Rey, A. Hungria, C. Duran-Valle, M. Faraldos, A. Bahamonde, J.A. Casas, J.J. Rodriguez, Appl. Catal. B Environ. 181 (2016) 249–259.
[37] F.J. Rivas, V. Navarrete, F.J. Beltran, J.F. Garcıa-Araya, Appl. Catal. B Environ. 48 (2004) 249–258.
[38] G. Pliego, J.A. Zazo, J.A. Casas, J.J. Rodriguez, J. Environ. Chem. Eng. 2 (2014) 2236–2241.
[39] Y. Peng, D. Fu, R. Liu, F. Zhang, X. Xue, Q. Xu, X. Liang, Appl. Catal. B Environ. 79 (2008) 163–170.
[40] H. Jin, X. Tian, Y. Nie, Z. Zhou, C. Yang, Y. Li, L. Lu, Environ. Sci. Technol. 51 (2017) 12699–12706.
[41] C. Yin, J. Cai, L. Gao, J. Yin, J. Zhou, J. Hazard. Mater. 305 (2016) 15–20.
[42] C.-H. Liao, S.-F. Kang, F.-A. Wu, Chemosphere 44 (2001) 1193–1200.
[43] G.V. Buxton, C.L. Greenstock, W.P. Helman, A.B. Ross, J. Phys. Chem. Ref. Data 17 (1988) 513–886.
[44] J.E. Grebel, J.J. Pignatello, W.A. Mitch, Environ. Sci. Technol. 44 (2010) 6822–6828.
[45] G. Pliego, N. Xekoukoulotakis, D. Venieri, J.A. Zazo, J.A. Casas, J.J. Rodriguez, D. Mantzavinos, J. Chem. Technol. Biotechnol. 89 (2014) 814–818.
[46] J.A. Zazo, G. Pliego, P. García-Muñoz, J.A. Casas, J.J. Rodriguez, Appl. Catal. B Environ. 192 (2016) 350–356.
[47] C. Moreno-Castilla, M.A. Ferro-Garcia, J.P. Joly, I. Bautista-Toledo, F. Carrasco-Marin, J. Rivera-Utrilla, Langmuir 11 (1995) 4386–4392.
[48] J.L. Figueiredo, M.F. Pereira, M.M. Freitas, J.J. Orfao, Carbon 37 (1999) 1379–1389.
[49] H. Darmstadt, C. Roy, S. Kaliaguine, Carbon 32 (1994) 1399–1406.
[50] E. Paparazzo, J. Elect, Spectrosc. Related Phenom. 43 (1987) 97–112.
[51] Y.-S. Lee, H.-T. Kim, K.-O. Yoo, Ind. Eng. Chem. Res. 34 (1995) 1181–1188.
[52] J.G. Terlingen, J. Feijen, A.S. Hoffman, J. Colloid, Interface Sci. 155 (1993) 55–65.